Summary

Erosive wear occurs in many fields of materials handling technology; e.g., during transportation of bulk materials or suspensions, when particles collide with the walls of material handling components such as ducts or pumps. The severity of wear is closely determined by both, component materials and the flow conditions in the medium. Hence a prediction of the wear needs a combination of Computational Fluid Dynamics (CFD) and a Finite Element Method (FEM) that offers realistic simulation of erosion in materials handling components.

This paper presents an approach to calculate particle trajectories of a suspension flow. The particle trajectories of a suspension flow are simulated using CFD and experimentally validated. The presented results are part of a project attributed to the VDMA Pumps + Systems which includes the erosion simulation using FEM [1].

The presented approach contributes to the pre-development of material handling components such as pumps and offers valuable assistance to manufactures. This allows a time- and cost-efficient development of wear-resistant components.

1. Introduction

Erosive wear occurs in many fields of materials handling technology; e.g., during transport of bulk materials or suspensions when particles collide with the walls of material handling installations such as ducts or pumps. These collisions cause removal of material and hence lead to a reduced availability of the components. The resulting economic damage is significant for system operators. By increasing the durability of such components in fluid power systems, manufacturers will have a significant competitive advantage [2].

The wear resistance of components in bulk materials or suspension flows depends on many parameters. This makes a purely experimental investigation expensive. In a project attributed to the VDMA Pumps + Systems (project no. 17400) a holistic approach is used for the simulation of solid particle erosion due to suspension flows [1]. Therefore, a combination of CFD and FEM is used for the simulation of erosion wear. At first, the particle trajectories of a two-phase suspension flow are simulated using CFD. The particle trajectories – including impact angle, velocity, and hit location – serve as input parameters for the erosion model. The erosion wear due to impacting particles is calculated by using FEM. With CFD and FEM it is possible to optimize the components already during their pre-development without experiments.

In this project (no. 17400) the authors were responsible for the CFD simulations and the experiments. Therefore, this paper presents the CFD model to calculate particle trajectories due to suspension flows. Thereby, a change in the component geometry due to material removal is not computed and has no influence on the suspension flow. This is a justified assumption for initiating erosion.

The paper is subdivided into 4 major parts: (i) At first, we give an overview on the various approaches to solve the described problem; (ii) Afterwards, the test rig for validation and the used model are presented; (iii) Then the results of the simulations and experiments are following; (iv) the paper closes with a conclusion and an outlook.

2. A Short Survey of Suspension Flows

A suspension is a heterogeneous mixture of a liquid (fluid) and solids (particles) dispersed therein. Suspension flows - or more generally known as multi-phase flows - are divided into *locally homogeneous flows* (LHF) and *separated flows* (SF) [3]. LHF-models use a quasi-single phase continuum. Thereby, the thermodynamic quantities and the material law of the quasi-single phase will be adjusted to model a multi-phase flow. Both phases must be in thermodynamic and mechanical equilibrium [4]. Buggish [5] and Shuen et al. [6] use LHF-models to calculate suspension flows with very high particle volume fraction, so-called pastes. The absence of momentum transfer between the phases of LHF-models leads to an over-estimation of the dispersion of the particles [7], [8].

In contrast to LHF-models SF-models calculate the phase interaction. Gosman et al. [9] divide SF-models into *continuum formulation models* (CF), *continuous particle models* (CP) and *discrete particle models* (DP). Usually the fluid is described as a continuum in the *Euler-approach* (EA). The particles are treated as a continuum or discrete in a *Lagrange*-approach (LA). In CF, all phases are solved simultaneously in EA. Therefore, the continuum hypothesis for the phases must be satisfied. To satisfy the continuum hypothesis the number of particles or fluid molecules must be sufficiently large in a control volume. The continuum hypothesis is verified if the *Knudsen* number is $Kn \leq 0.01$. The *Knudsen* number is a ratio of mean free path of the fluid molecules to a characteristic length of the flow. If the phase is described in LA, the continuum hypothesis does not have to be satisfied, but each particle or fluid molecule must be tracked. CP and DP differ in the description of the properties of the disperse phase. CP uses statistically distributed properties of the particles. In DP, the particles have localized properties. The particles in DP can be represented as mass points without water displacement or as an assembly of spheres [10].

A combination of EA and LA for disperse phase is shown in [11]. Finally, the approaches are mentioned, which are used by [12], [13], [14]. In these cases the fluid phase is performed also in LA.
According to [4], [15] DP is the most common approach. In combination with a stochastic collision model [16], DP is the only model which can simulate practice-oriented problems for suspension flows in reasonable time. Following this argumentation we applied a DP approach in this paper. In the following section, DP is discussed in detail.

In DP, the particle trajectories are calculated with the *Newtonian* equation of motion. Hereby, the acting forces on the particles are divided into volume forces and surface forces. Volume forces occur due to gravitational, magnetic and electric fields and refer to long-distance effect. Surface forces can be subdivided into fluid-particle interaction forces and proximity effect. There is a big variety of fluid-particle interaction forces. Extensive literature on these forces can be found in [15], [17], [18]. The contact forces due to collisions between the particles or adjacent walls and the adhesive forces by material or non-material compounds are proximity effects [15].

The collision of particles is numerically computed in two steps. First, the collision of particles is detected deterministically or stochastically. In the second step the momentum transfer due to the collision is calculated either by a so-called hard-sphere model or a soft-sphere model.

Based on the particle volume fraction or the concentration Φ and the *Stokes* number of the particles, respectively, the decision is being made which forces in the suspension flow have to be modelled. The concentration represents the ratio of the volume of all particles to the total volume. The *Stokes* number of the particles is the ratio of the characteristic time of the particles to a characteristic time of the flow. Thereby a suspension is divided into dilute and dense on the basis of *Stokes* number and concentration [19], [20]. A dense suspension has a high concentration $\Phi > 10^{-3}$ and the collision between the particles have to be considered. In this regime the momentum transfers between the fluid and particles as soon as the particles themselves are computed. The particle collisions in dilute suspensions $10^{-6} < \Phi \leq 10^{-3}$ are negligible but the turbulence has an influence on the particle motion vice versa. For concentrations $\Phi < 10^{-6}$ the disperse phase has no influence on fluid turbulence [21]. The *Stokes* number is used to characterize the influence of turbulence. The influence of fluid turbulence on the particle movement is called turbulent dispersion. The production and damping of the fluid turbulence due to the particle movement is called turbulence modulation [22], [23].

3. Experimental and numerical Set-Up

In this chapter the used model of the suspension flow and the test rig for the validation will be presented.

Test Rig

The test rig consists of a closed loop with cooling and adjustable static pressure to avoid cavitation. The volume of the test rig is about $850\,\mathrm{l}$. Figure 1 shows the flow direction and the infrastructure of the test rig with motor, pump, pressure vessel and measuring section. The particles are weighted and added to the flow. The suspension is a mixture of water and corundum particles. The particles are preconditioned. Preconditioned corundum particles change their shapes and properties slowly compared to new corundum particles.

A quasi-stationary operating point is set with a speed controlled pump and monitored. In addition, the flow field in the measuring section is measured for particle-free flow with the particle image velocimetry (PIV). The particle trajectories of dilute suspensions are investigated by means of particle tracking velocimetry (PTV). During the wear tests with dense suspensions, a measuring

of the particle trajectory is impossible. But after the experiment, the material loss of the specimen is determined with a precision balance to verify the wear resistance of the materials.

Figure 1 shows also a sectional drawing of the measuring section. The measuring section is optically accessible and arranged vertically to avoid particle deposition. The measuring section is rectangular with a width of $W = 25\,\mathrm{mm}$ and a height of $H = 70\,\mathrm{mm}$. A nozzle in front of the measuring section reduces the circular cross-section to the rectangular measuring section. A diffusor behind the measuring section is used to minimize the losses.

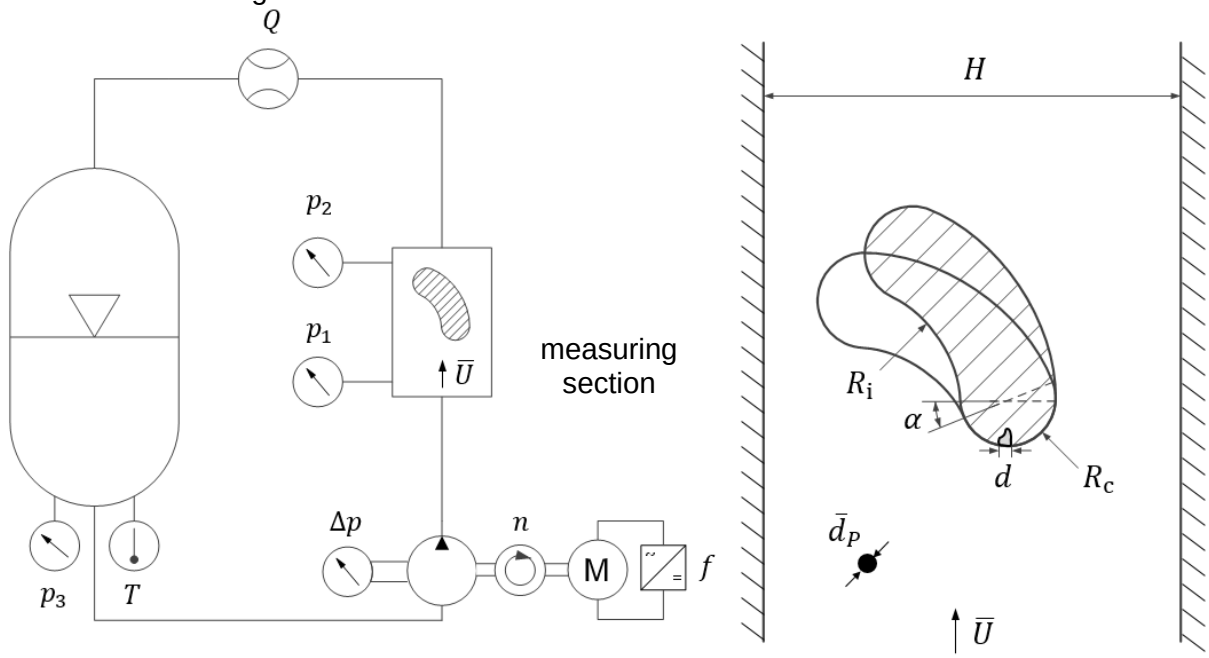

Figure 1: Hydraulic diagram of the Test Rig with sensors and sectional drawing of the measuring section. The absolute pressure in the pressure vessel p_3 and measuring section (p_1, p_2), the differential pressure across the pump Δp, the temperature T, the volume flow Q, the rotational speed of the pump n and the frequency of the frequency converter f are measured during a quasi-stationary operating point.

The specimen can be rotated to change its angle of attack α in the flow. An additional pressure vessel is used to reduce the water gauge in the measuring section to change the specimen without losing the suspension. The shape of the specimen is a circular arc segment with a pressure and a suction side like a blade. The size of the specimen and the measuring section are a compromise of power consumption of the test rig and technical measurement reasons. Furthermore, the wear of the specimen must be independent of its size. To avoid the influence on the wear, the mean diameter of the particles $100\,\mu\mathrm{m} \geq \bar{d}_P \geq 50\,\mu\mathrm{m}$ is much smaller than the characteristic dimensions of the specimen ($R_\mathrm{i} = 10\,\mathrm{mm}$, $R_\mathrm{c} = 4\,\mathrm{mm}$).

Model of the Suspension Flow

As mentioned earlier, the suspension flow is modelled be means of a DP approach. The particles are material points and have no water displacement. An examination with a light microscope shows that the particles are not spherical. However, for the calculation of the forces, i.e. the drag, the particles are assumed to be spheres. All forces acting on the particles are listed in table 1. The fluid (water) is modelled as a continuum using a turbulence model. The domain of the model includes the rectangular measurement section with specimen and the nozzle as described before. In order to reduce the computing time, the model has no diffusor. The particles are randomly distributed at the inlet with a normally distributed diameter of the particles. The particles have the same velocity and direction as the flow at the inlet. The grid- and turbulence-study is carried out

for particle-free flow and validated with PIV, as can be seen in figure 2. The properties, settings and the changeable parameters of the model are listed in table 1.

Due to limited computational resources, it is impossible to simulate every particle in the test rig. For example, a volume of $850\,\mathrm{l}$ with a concentration of $\Phi = 1\%$ and a mean particle diameter of $\bar{d}_P = 100\,\mu\mathrm{m}$ contains about 10^{10} particles. However, it is possible to get realistic particle trajectories with the stochastic collision model if these three constraints are met: (i) The concentration must be small enough so that binary collisions dominate; (ii) The number of the particles needs to allow for stochastic calculations; (iii) The velocity of the colliding particles is not correlated.

Two results of a preliminary investigation are anticipated here. The used DP generates plausible results up to a particle volume fraction of $\Phi = 2\%$. With gradual increase of the order of the number of particles from 10^5 to 10^6, there is only a marginal change of the particle trajectories.

	Fluid (water)	**Particle**
Properties	Element Number $\approx 2.8 \times 10^6$ $mean(y^+) \approx 2.6, max(y^+) \approx 9$ Continuum	Particle Number $= 10^5$ Material Points
Physically effects	Stationary Gravity Incompressible Newtonian Fluid Menter SST-turbulence-model	Drag: Schiller, Naumann Buoyancy: Density Difference Virtual mass coefficient $= 0.5$ Pressure gradient Turbulent Dispersion: Gosman, Ioannides Collision: Sommerfeld
Boundaries	Velocity inlet Pressure outlet Rough Wall: Sommerfeld, Frank	Velocity and direction of flow at inlet Randomly distributed at inlet Fully elastically collisions
Parameter	Mean velocity Concentration Angle of attack of the specimen	Particle diameter (as distributed parameter) Particle density

Table 1: Properties and settings of the CFD-model

4. Results and Discussion

The suspension flow is solved with a DP as described in chapter 2. The model is being validated in three steps with the test rig shown in figure 1. The first step is to validate the computed flow field of the particle-free flow. The comparison of the predicted particle trajectories in dilute suspension with the experiment is the second step. The last step is the wear tests with dense suspensions to compare the wear resistance of different materials, which can be seen in [1]. Furthermore, the wear pattern is an indicator for a realistic simulation of the particle trajectories in dense suspensions.

Flow Field

The stationary flow field without particles is validated by means of PIV. Figure 2 shows the best (II) and the worst (I) match between experiment and simulation. The relative deviation between the flow velocity of the experiment u_E and simulation u_S is shown on the left side of the figure. On the right side the relative measuring error ($\delta_\mathrm{sys}, \delta_\mathrm{stat}$) of the PIV-system is depicted.

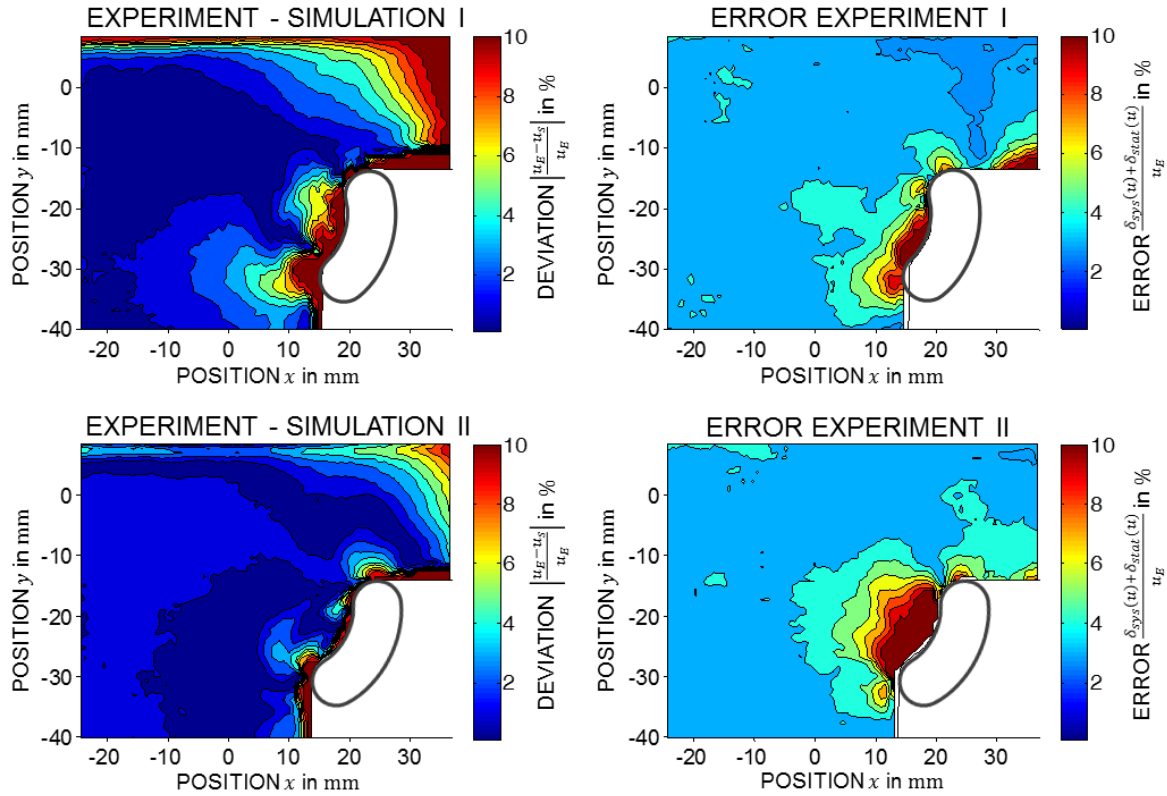

Figure 2: Left side, relative deviation between experiment and simulation for configuration I ($\overline{U} = 15\ \mathrm{m/s}$, $\alpha = 45°$) and II ($\overline{U} = 20\ \mathrm{m/s}$, $\alpha = 30°$). Right side, relative measuring error of configuration I and II.

The uncertainty analysis of the measuring error is explained in [1]. The area under and right to the specimen is cut off (white areas) because the laser light of the PIV-system comes from above and the specimen casts a cloud over the area under itself. The right side is cut off because the PIV-system is not able to dissolve the transient area of the wake.

The relative deviation between experiment and simulation is smaller than the relative measuring error for a large area. The differences increase where the channel is narrowing and on the surface of the specimen. An evaluation on the surface of the specimen is difficult due to the camera resolution and the reflections on the specimen surface.

Particle trajectories

The particle trajectories for dilute suspensions are measured by PTV. Thereby, the laser sheet is also introduced from above into the measuring section and the high speed camera is directed perpendicular to the specimen. Figure 3 shows the measured and calculated particle trajectories from the best (II) and worst (I) match between them. The mean velocity of the configuration II is $\overline{U} = 12\ \mathrm{m/s}$, the concentration is about $\Phi \approx 0.02\%$ and the angle of attack is $\alpha = 0°$.Configuration I has $\overline{U} = 6\ \mathrm{m/s}$, $\alpha = 0°$ and the same concentration. The top of figure 3 contains the particle trajectories of the simulation and the experiment of configuration II. At the bottom there is the relative deviation between experiment and simulation of configuration I and II. Long particle trajectories as seen in the simulation could not be calculated with the experimental data. On the photo series of the high speed camera, the particles disappear and reappear. For two reasons the particles do not reflect the laser light into the camera: The first reason is that the particles leave the laser sheet and the second reason is that the particles scatter the light in the wrong direction because of their shapes.

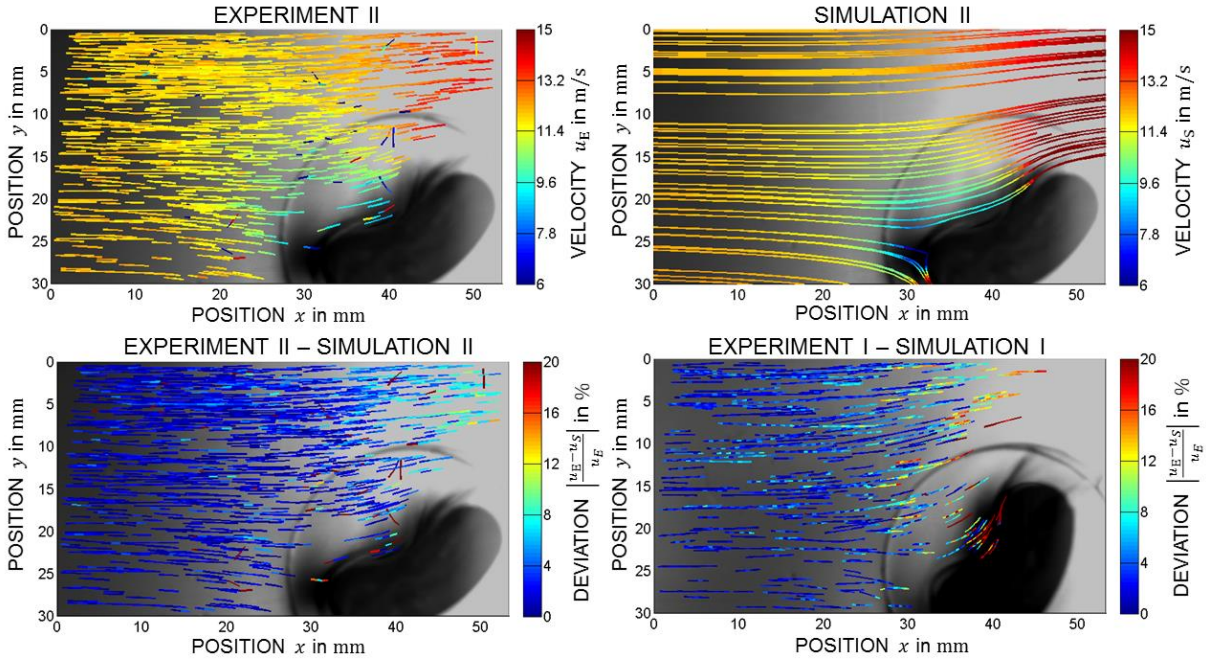

Figure 3: Particle trajectories of dilute suspensions for two configurations. The measured and computed velocity of the particles for configuration II are shown on top and the relative deviation between simulation and experiment for configuration I and II are shown at the bottom of the figure.

Wear is determined mainly on the front of the specimen and on the channel walls. Therefore the area in front of the specimen should be well reproduced from the simulation. The relative deviation between simulation and experiment is below 3% in the area in front of the specimen. The measuring error depends on the particle velocity and the camera resolution. The relative measuring error is about $3\ \%$ up to $5\ \%$. The uncertainty analysis is in [1]. There are only a few trajectories in front of the specimen which are not plausible. The deviation between simulation and experiment increases where the channel is narrowing, as seen by the PIV experiments. However, for a wide area in front of the specimen the particle trajectories between simulation and experiment are similar.

As aforementioned a measurement of the particle trajectories of dense suspensions is impossible. However, the wear observed in the test rig and shown in figure 4 is an indicator for a realistic simulation of the particle trajectories. The wear begins where the computed impact velocity is high. This wear pattern occurs again and again so that the particle trajectories seem to be right. In this preliminary test, the specimen holder consists of brass. Afterwards, the holder was produced of high-grade steel for the series of tests. Additionally, the holder was replaced periodically to avoid an influence on the flow and the wear of the specimen.

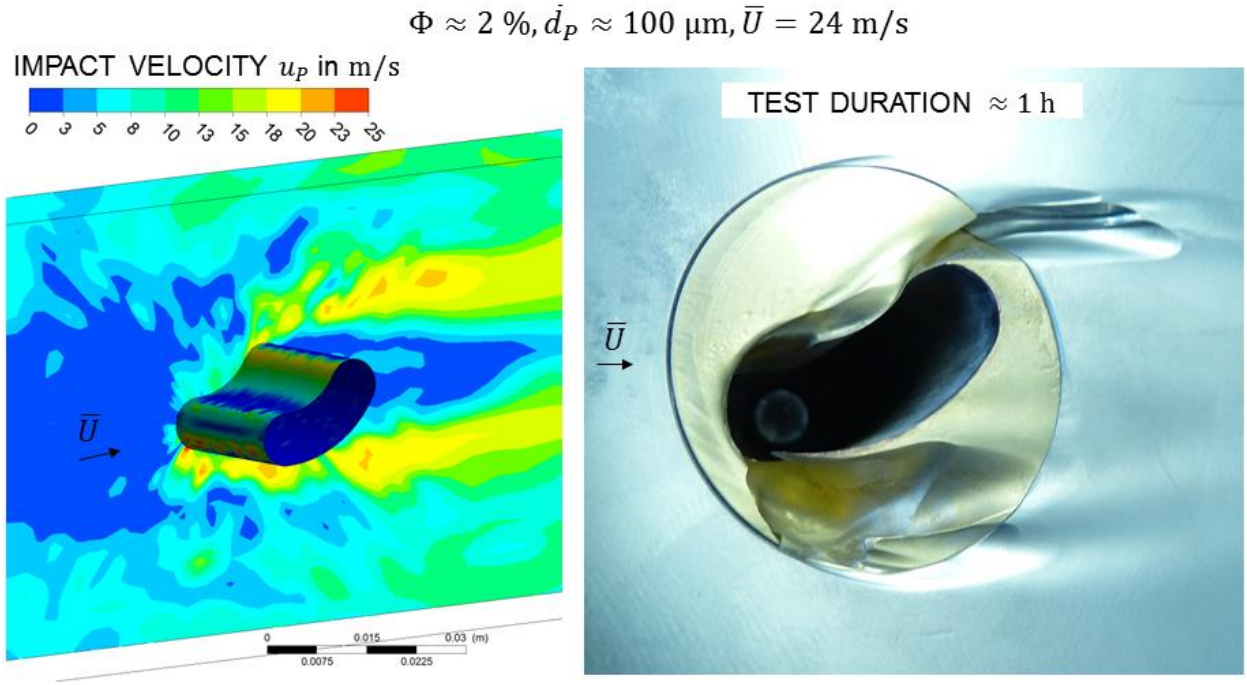

Figure 4: Left side, simulation of the impact velocity of the particles. Right side, wear of the channel wall and the specimen holder after one hour.

5. Conclusion and Outlook

The particle trajectories of a suspension flow are simulated for practice-oriented problems in reasonable time. The CFD simulations of particle-free flows and dilute suspensions were validated by a test rig. Furthermore, the wear pattern due to the wear tests show realistically calculated particle trajectories in dense suspensions.

The calculated particle trajectories on the specimen – including impact angle, velocity, and hit location – serve as input parameters for the erosion model in [1]. The wear tests are used to validate the whole approach with the presented CFD-model and the erosion model in [1]. The material removal was calculated about 4 up to 5 times greater than in the experiment. A possible reason for this inaccuracy is a higher concentration of the suspension in the simulations as in the experiments. The particle concentration in the measuring section is not measured. Hence, particle sedimentation in the test rig is not excluded. Another possible reason is the inaccuracy of the erosion model.

To increase the accuracy of the whole approach the concentration of the suspension should be measured in the measuring section. Furthermore, the erosion model can be improved with the worn specimens. Micrographs of a specimen show similar erosion to a FEM model. But the material removal of different used FEM models varies. The micrographs of the specimens must be repeated on different specimen to validate the used FEM models in [1].

Acknowledgement

The presented results were developed by the Chair of Fluid Systems (FST), Technische Universität Darmstadt. The project is attributed to the VDMA Pumps + Systems and funded by Arbeitsgemeinschaft Forschungsvereinigungen Otto von Guericke e.V. (AIF), project no. 17400.

References

[1] A. Krebs, I. Budde, S. Schmauder and P. F. Pelz, “Simulation des Erosionsbeginns von MMC-Werkstoffen,” VDMA, Frankfurt, 2015.

[2] P. F. Pelz and S. Schmauder, “Numerische Vorausberechnung des Erosionsbeginns durch auftreffende Partikel auf Metallmatrix-Verbundwerkstoffe,” AiF-gefördertes IGF-Vorhaben 17400, Fachverband Pumpen und Systeme im VDMA, TU Stuttgart & TU Darmstadt, 2011.

[3] G. M. Feath, “Recent advances in modeling particle transport properties and dispersion in turbulent flows,” *ASME • JSME Thermal Engineering Joint Conference Proceedings,* vol. 2, 1983.

[4] A. Matysiak, Euler-Lagrange Verfahren zur Simulation tropfenbeladener Strömung in einem Verdichtergitter, Hamburg: Helmut-Schmidt-Universität / Universität der Bundeswehr Hamburg, 2007.

[5] J. Götz, D. Müller, H. Buggisch and C. Tasche-Lara, “NMR flow imaging of pastes in steady-state flows,” *Chemical Engineering and Processing: Process Intensification,* vol. 33, no. 5, pp. 385-392, 1994.

[6] H. Buggisch, “Über das zeitabhängige Fließverhalten von Pasten,” *Chemie Ingenieur Technik,* vol. 67, pp. 1148-1149, 1995.

[7] J. Shuen, L. Chen and G. Faeth, “Evaluation of a stochastic model of particle dispersion in a turbulent round jet,” *AIChE Journal,* vol. 29, no. 1, pp. 167-170, 1983.

[8] J. Shuen, “A theoretical and experimental study of turbulent particle-laden jets,” Technical Report NASA-CR-168293. NASA - Lewis Research Center, Cleveand, 1983.

[9] A. Gosman and J. Johns, “Computer Analysis of Fuel-Air Mixing in Direct-Injection Engines,” SAE-Paper 800091, 1980.

[10] D. Morrison and W. Wu, “Experimental Validation of the discrete element method (DEM),” in *Iron Ore*, Perth, 2007.

[11] C. Grüner, Kopplung des Einzelpartikel- und des Zwei-Kontinua-Verfahrens für die Simulation von Gas-Feststoffströmungen, Dortmund: Universität Dortmund, 2004.

[12] X. Bian and M. Ellero, “A splitting integration scheme for the SPH simulation of concentrated particle suspensions,” *Computer Physics Communications,* vol. 185, pp. 53-62, 2014.

[13] N. Martys, W. George, B. Chun and D. Lootens, “A smoothed particle hydrodynamics-based fluid model with a spatially dependent viscosity: application to flow of a suspension with a non-newtonian fluid matrix,” *Rheologica Acta,* vol. 49, pp. 1059-1069, 2010.

[14] A. Potapov, M. Hunt and C. Campbell, “Liquid-solid flows using smoothed particle hydrodynamics and the discrete element method,” *Powder Technology,* vol. 116, pp. 204-213, 2001.

[15] B. Epple, R. Leithner, W. Linzer and H. Walter, Simulation von Kraftwerken und Feuerungen, Germany: Springer-Verlag/Wien, 2012.

[16] M. Sommerfeld, “Validation of a stochastic Lagrangian modelling approach for interparticle collisions in homogeneous isotropic turbulence,” *International Journal of Mulitphase Flow,* pp. 1829-1858, May 2001.

[17] S. Hodgson, Turbulence modulation in gas-particle flows a comparison of selected models, Ottawa: National Library of Canada = Bibliothèque, 2001.

[18] J. Shirolkar, C. Coimbra and M. Mcquay, “Fundamental aspects of modeling turbulent particle dispersion in dilute flows,” *Progress in Energy and Combustion Science,* vol. 22, pp. 363-399, 1996.

[19] C. Crowe, “REVIEW-Numerical Models for Dilute Gas-Particle Flows,” *Journal of Fluids Engineering,* vol. 104, pp. 297-303, 1982.

[20] S. Elghobashi, “Particle-laden turbulent flows: direct simulation and closure models,” *Applied Scientific Research,* vol. 48, pp. 301-314, 1991.

[21] S. Elghobashi, “On Predicting Particle-Laden Turbulent Flows,” *Applied Scientific Research,* vol. 52, pp. 309-329, 1994.

[22] C. Liu, “Turbulent dispersion of dynamic particles,” *Journal of the Meteorological Society of Japan,* vol. 13, no. 4, p. 399–405, 1956.

[23] M. Hillers, Modellierung der Turbulenzmodulation einer hochbeladenen reaktiven Zweiphasenströmung am Beispiel des Zementherstellungsprozesses, Duisburg: Universität Duisburg, 2008.